Journal of Cellular Biochemistry 100:474–486 (2007)

Iron Chelation Study in a Normal Human Hepatocyte Cell Line Suggests That Tumor Necrosis Factor Receptor-Associated Protein 1 (TRAP1) Regulates Production of Reactive Oxygen Species

Chang-Nim Im,[1] Jae-Seon Lee,[2] Ying Zheng,[1] and Jeong-Sun Seo[1]*

[1]Department of Biochemistry and Molecular Biology, ILCHUN Molecular Medicine Institute MRC, Seoul National University College of Medicine, Seoul 110-799, Seoul, Korea
[2]Laboratory of Functional Genomics, Korea Institute of Radiological and Medical Sciences, Seoul 139-706, Korea

Abstract Iron is an essential component of many proteins, and has crucial roles in the proper functioning of proteins involved in cellular respiration, proliferation, and differentiation. It has been recently reported that the deferoxamine (DFO), an iron chelator, induces mitochondrial dysfunction, characterized by an attenuation of oxidative phosphorylation, as well as senescence-like cellular morphology. However, the effects of DFO on mitochondrial heat shock proteins (HSPs) remain poorly understood. In this study, we examined the effect of DFO on tumor necrosis factor receptor-associated protein 1 (TRAP1), a representative mitochondrial HSP, in a normal human hepatocyte cell line, Chang cells. DFO specifically decreased TRAP1 levels, increasing reactive oxygen species (ROS) and caveolin-1 (Cav-1), a marker protein of senescence. To examine whether these effects of DFO are reversed, we established TRAP 1-overexpressing Chang cells. DFO treatment to TRAP1-overexpressing cells resulted in decreases in levels of ROS, Cav-1, glutathione peroxidase (GPX), and manganese superoxide dismutase (MnSOD) levels as well as senescence-associated β-galactosidase (SA β-gal) activity. These results suggest that TRAP1 might play a role in protecting mitochondria against damaging stimuli via decrease of ROS generation. J. Cell. Biochem. 100: 474–486, 2007. © 2006 Wiley-Liss, Inc.

Key words: deferoxamine; mitochondria; TRAP1; ROS

Iron is an essential element involving in the electron transfer events associated with ATP synthesis [Robbins and Pederson, 1970; Nyholm et al., 1993; Oexle et al., 1999]. Iron is normally internalized via receptor-mediated endocytosis, in which transferrin, a non-heme beta-globin, binds to transferrin receptor (TfR) [Richardson and Baker, 1990]. It has been reported that TfR expression can be regulated by several mechanisms, including iron response elements (IRE) in 3′ UTR, which iron regulatory protein binds to and regulates the stability of TfR mRNA, as well as the iron status of the cell. Intracellular iron levels appear to determine TfR at the post-transcriptional level, whereas transferrin is regulated at the transcriptional level [Kuhn et al., 1990; Koeller et al., 1991]. Also, cellular iron availability has been shown to regulate the expression of proteins involved in the growth and functions of cells such as nitric oxide synthetase and PKC-beta [Alcantara et al., 1994; Weiss et al., 1994]. Therefore, the maintenance of cellular iron homeostasis is crucial, and improper iron regulation has been implicated in diseases such as cirrhosis and hepatoma. Deferoxamine (DFO), which is produced by *Streptomyces pilosus*, binds to iron and acts as an iron chelator in cells [Keberle, 1964]. DFO has been shown to exert an anti-proliferative effect on certain

Grant sponsor: 2005 BK21 project for medicine, dentistry, and pharmacy.

*Correspondence to: Jeong-Sun Seo, Department of Biochemistry and Molecular Biology, ILCHUN Molecular Medicine Institute MRC, Seoul National University College of Medicine, 28 Yongondong, Chongnogu, Seoul 110-799, Korea. E-mail: jeongsun@snu.ac.kr

Received 14 March 2006; Accepted 15 June 2006

DOI 10.1002/jcb.21064

© 2006 Wiley-Liss, Inc.

cancer cell lines, including hepatoma, leukemia, and neuroblastoma cells [Lederman et al., 1984; Kontoghiorghes et al., 1986; Brodie et al., 1993; Fan et al., 2001]. Also, DFO regulates the expression of many genes such as cytochrome c oxidases and ubiquinone oxidoreductase involving in ATP synthesis [Ye and Connor, 1999]. For example, DFO induces a series of changes such as G1 cell cycle arrest, a decrease in the levels of ATP, and a flattening of cellular morphology in a normal human hepatocyte cell line, Chang cells. These DFO-associated alterations have been attributed, at least in part, to mitochondrial defects such as inhibition of complex II activity through a down-regulation of iron-sulfur subunit [Yoon et al., 2003, 2004].

Mitochondria are vitally important organelles, in which the majority of the ATP serving as the primary energy source of the cell is synthesized, via oxidative phosphorylation and electron transfer. The mitochondria are surrounded by a double-membrane system, which consists of inner and outer membranes. Folds in this inner membrane, called the cristae, extend into the matrix [Hatefi, 1985; Saraste, 1999]. Many different stresses appear to target this organelle, which result in deleterious effects such as apoptosis and cell cycle arrest. Cells adapt to these stresses via the utilization of different defense mechanisms. For example, heat shock proteins (HSPs) play a pivotal role in cellular defense. The HSPs are evolutionarily-conserved proteins, which function not only as chaperones, but also in diverse mammalian cellular processes [Goldberg, 2003]. Previously, we reported that cytosolic HSP70 protects cells against heat shock-induced apoptosis [Li et al., 2000]. In addition, the disruption of hsp70.1 gene is vulnerable to osmotic stress and infarction [Lee et al., 2001; Shim et al., 2002]. Besides cytosolic HSP70, some HSPs which are present in the mitochondria function as chaperones for mitochondrial proteins. These mitochondrial chaperones include HSP60 (HSP60 family member), Mot-2 (HSP70 family member), and tumor necrosis factor receptor-associated protein 1 (TRAP1) (HSP90 family member), and several others. A recent report has shown that mitochondrial HSP60 is associated with resistance to oxidative stress in *Saccharomyces cerevisiae* [Cabiscol et al., 2002]. It has been demonstrated that overexpression of Mot-2 results in a reduction in the accumulation of ROS in PC12 cells after glucose deprivation [Liu et al., 2005]. Recent reports have shown that *Dictyostelium discoideum* TRAP1 (Dd-TRAP1) is associated with spore differentiation occurring during the development, and plays a role in prestarvation response in *Dictyostelium discoideum* [Morita et al., 2002, 2004, 2005]. A study by Masuda [2004] demonstrated the involvement of TRAP1 in β-hydroxyisovalerylshikonin (β-HIVS)-induced apoptosis. Prevention of the suppression of TRAP1 expression by β-HIVS by the antioxidant, N-acetyl-cysteine suggests the involvement of reactive oxygen species in the regulation of TRAP1 expression.

In this study we attempted to ascertain whether DFO might exert some influence on mitochondrial HSPs in a normal human hepatocyte cell line, Chang cells. We found that levels of TRAP1, but not HSP60 and Mot-2, decrease dramatically in DFO-treated Chang cells. In addition, using TRAP1-overexpressing Chang cells, we demonstrated that TRAP1 overexpression reduces the DFO-associated ROS generation, along with decreases in senescence-associated-β-galactosidase (SA-β-gal) activity, caveolin-1 (Cav-1), glutathione peroxidase (GPX), and manganese superoxide dismutase (MnSOD) levels. These findings suggest that DFO negatively regulates the levels of TRAP1, thereby affecting an augmentation of ROS generation.

MATERIALS AND METHODS

Cell Culture and Deferoxamine (DFO) Treatment

Chang cell, a normal human hepatocyte cell line (kindly provided by Dr. Gyesoon Yoon at Ajou University, Korea) was cultured in Dulbecco's Modified Eagle's Medium (DMEM; JBI., Korea) supplemented with 10% (v/v) fetal bovine serum (FBS; JBI., Korea), 100 U/ml of penicillin (Sigma), and 100 μg/ml of streptomycin (Sigma) in an incubator at 37°C, under an atmosphere containing air and 5% CO_2. The cells (5×10^5) were seeded into 100-mm dishes, cultured overnight in DMEM containing 10% FBS DMEM, and treated with 0.5 mM DFO (Sigma) for the indicated time periods. In some cases, N-acetyl-L-cysteine (NAC, Sigma) was added at a concentration of 1 or 10 mM, either with or without DFO treatment.

Electron Microscopy

The cells were fixed with 2.5% glutaraldehyde, and post-fixed in 1% buffered osmium

tetroxide. After dehydration with a graded ethanol series and embedding in Epoxy resin (Poly bed 812 kit), ultra-thin sections were prepared using an ultra-microtome (RMC products-MTXL) equipped with a diamond knife. Heavy metal staining was conducted with 4% uranyl acetate and lead citrate solutions, and samples were visualized via electron microscopy (Tokyo, Japan) at 60 kV. At least two blocks per sample was made and 4–5 sections per grid were observed under electron microscope. At least seven cells per section were randomly selected and mitochondria per cell were counted under electron microscope. For estimating the relative length of mitochondria, mitochondrial photographs were obtained under electron microscope. After their images were scanned, the relative ratio of length to control (i.e., length in DFO-treated sample vs. length in control sample) was calculated using the Image J program (National Institutes for Health). Two independent experiments were performed and each value was expressed as the mean values and standard deviations.

Western Blotting

The Chang cells were lysed in a buffer containing 50 mM Tris, pH 7.4, 150 mM NaCl, 1 mM EDTA, 1% Triton X-100, complete protease inhibitor cocktail (Roche), 1 mM phenylmethylsulfonyl fluoride, and 1 mM NaF, for 30 min on ice. The cell lysates were centrifuged, quantitated with protein assay reagent (Bio-Rad), and subjected to sodium dodecyl sulfate-polyacrylamide gel electrophoresis (SDS–PAGE). The proteins were transferred to nitrocellulose membranes (S&S). The membranes were blocked with 5% (w/v) nonfat dry milk in 1× Tris buffered saline containing 0.1% Tween-20 (TBS-T), for 1 h at room temperature. Each of the proteins was detected with its specific antibody (anti-mouse TRAP1 antibody from NeoMarkers, anti-goat HSP60 and anti-mouse β-actin antibodies from Santa Cruz Biotechnology, and anti-mouse GPX, anti-rabbit Mot-2, anti-rabbit MnSOD, and anti-rabbit Cu/ZnSOD antibodies from Stressgen, anti-mouse Cav-1 from Transduction laboratories). The antibody-antigen complex was detected with horseradish peroxidase-conjugated secondary antibody (Santa Cruz Biotechnology), and visualized via the standard chemiluminescence technique, which was conducted in accordance with the manufacturer's provided instructions (Pierce). Images were generated on LAS 3000 (Fujifilm).

Reverse Transcription-PCR

Total RNA was purified with TRI® reagent (Sigma), again in accordance with the manufacturer's provided instructions. After treating DNase I (Sigma) to 1 μg of total RNA according to manufacturer's instructions, first-strand cDNA was synthesized with reverse transcriptase (Invitrogen) and 1 μg of oligo-dT primer (Invitrogen). Each 1–3 μl cDNA of the sample was amplified via 30–35 cycles of PCR, as follows: denaturation for 30 s at 94°C, 30 s of annealing at 60°C, and a final 30 s of extension at 72°C, using specific primers against TRAP1 (sense: 5′-CCGTCCATGTTTGATGTGAG-3′ and antisense: 5′-CAAACTCACGAAGGTGCAG-3′ from accession no. NM_016292), Hsp60 (sense: 5′-CACCGTAAGCCTTTGGTCAT-3′ and antisense: 5′- CAATGCCTTCTTCAACAGCA-3′ from accession no. NM_002156), Mot-2 (sense: 5′-GCGAAAGAAGGAACGAGTTG-3′, and antisense: 5′-TGCAGCTGAAAAATGACAGG-3′ from accession no. NM_004134), and β-actin (sense: 5′-AAATCTGGCACCACACCTTC-3′, and antisense: 5′-AAAGCCATGCCAATCTCATC-3′ from accession no. BC014861). The specific PCR products were resolved on 1% agarose gels, and visualized via ethidium bromide staining.

MTT Assay

The cells were divided at a density of 5×10^3 cells/well on 24-well plates, and then maintained at 37°C in an incubator in a 5% CO_2 atmosphere. 3-(4, 5-dimethylthiazol-2-yl)-2, 5-diphenytetrazolium bromide (MTT) reagent (Sigma) was added to each well, to a final concentration of 0.5 mg/ml. After 4 h of incubation at 37°C in an incubator under a 5% CO_2 atmosphere, the solution was suctioned and 200 μl of dimethyl sulfoxide (Sigma) was added to each well. Absorption was then measured at a wavelength of 570 nm. After extraction with background value, the relative ratio to the control was represented in terms of mean values and standard deviations.

Mitochondrial Membrane Potential (MMP, ΔΨm)

ΔΨm was estimated using 5, 5′, 6, 6′-tetrachloro-1, 1′, 3, 3′-tetrathylbenzimidazole carbocyanide iodide (JC-1; Molecular Probes), in accordance with the manufacturer's instructions. In order to assess changes in the ΔΨm of the

DFO-exposed cells, the cells were incubated for 30 min with JC-1 (10 μg/ml), then washed in phosphate-buffered saline (PBS) (137 mM NaCl, 2.7 mM KCl, 10 mM phosphate buffer, pH 7.4); and visualized with a fluoromicroscope (Becton-Dickinson) at 590 and 527 nm, respectively.

Immunofluorescence Analysis

Chang cells were grown on sterile coverslips and incubated with 500 nM MitoTracker Orange CMTMRos (Molecular Probes) for 30 min, in accordance with the manufacturer's instructions. The cells were then fixed for 10 min with 3.7% formaldehyde in PBS and permeabilized for 10 min at room temperature with 0.2% Triton X-100. The cells were blocked for 1 h with 1% bovine serum albumin in PBS at room temperature. Anti-TRAP1 (NeoMarkers) monoclonal antibody was added to the cells, and incubated overnight at 4°C. The cells were washed in PBS and incubated for 1 h at 4°C with fluorescent isothiocyanate-conjugated anti-mouse IgG (Santa Cruz Biotechnology). After washing, the cells were stained with 0.4 mg/ml 4′, 6-diamidino-2-phenylindole (DAPI, Sigma) for 10 min at room temperature. Fluorescent images were acquired via confocal microscopy after mounting.

Subcellular Fractionation

The cytosolic and mitochondrial fractions were isolated with digitonin. In brief, the cells were lysed in lysis buffer (80 mM KCl, 250 mM sucrose, 200 μg/ml digitonin in PBS) for 5 min on ice. After 5 min of centrifugation at 10,000*g*, the supernatant was used as a cytosolic fraction. The pellets were resuspended in buffer containing 50 mM Tris-Cl (pH 7.5), 150 mM NaCl, 2 mM EDTA, 2 mM EGTA, 0.2% TritonX-100, and 0.3% NP-40, and incubated for 10 min on ice. The supernatants were used as a mitochondrial fraction after 5 min of centrifugation at 10,000*g*. Samples of each fraction were then quantitated using protein assay reagent (Bio-Rad). Monoclonal Cox IV antibody (Molecular Probe) was employed as a mitochondrial protein marker to ensure fractionation quality.

Stable Transfection

pcDNA3.1-TRAP1 was prepared via subcloning into the pcDNA3.1 plasmid, under the control of the EF1α-promoter (a gift from Macrogen, Inc., Korea) with the original pOTB7-TRAP1 vector (obtained from the Korea Research Institute of Bioscience and Biotechnology, Korea). The transfection of 2 μg plasmids into the Chang cells (1×10^6 cells) was conducted with Lipofectamine Plus reagent (Invitrogen), in accordance with the manufacturer's instructions. After 48 h of incubation, G418 (2 mg/ml, A.G. Scientific Inc.) was added to the culture medium in order to select the transfected cells. The clones were selected after 3 weeks, and maintained in medium containing G418 antibiotics for use in the experiments.

Reactive Oxygen Species (ROS) Measurement

Intracellular ROS levels in cells were measured using 5-(and-6)-carboxy-2′, 7′-dichlorodihydrofluorescein diacetate (DCF-DA, Molecular Probes). In brief, the cells were washed in PBS, trypsinized, then neutralized with PBS containing 0.5% FBS. After two washes with PBS and further centrifugation, the cells were resuspended in PBS with a concentration of 20 μM DCF-DA and incubated for 20 min in darkness at 37°C. After washing, the cells were resuspended in PBS, and the fluorescence was measured via flow cytometry (excitation at 488 nm, emission at 515–545 nm). Data represents mean fluorescence intensity for 10,000 cells per sample.

Senescence-Associated β-Galactosidase (SA- β-gal) Assay

Cells were grown overnight at a concentration of 1×10^5 cells per 60 mm dish, then treated either with or without 0.5 mM DFO for the indicated periods. The cells were fixed for 5 min in 3% formaldehyde at room temperature, washed twice in cold PBS, and then incubated overnight in freshly prepared SA-β-gal staining solution [40 mM citrate/phosphate buffer (pH 6.0) containing 1 mg/ml 5-bromo-4-chloroindol-3-yl β-D-galactopyranoside (American Bioanalytical), 5 mM potassium ferricyanide (Sigma), 5 mM potassium ferricyanide (Sigma), 150 mM NaCl, and 2 mM $MgCl_2$] at 37°C. The cells exhibiting substantial staining under a light microscope were considered to be positive, counted, and represented as a percentage of the total number of cells. Each value was expressed as mean ± SD.

Statistical Analysis

Student's *t*-tests were employed in order to compare the differences between two different groups. A *P*-value of <0.05 was considered statistically significant.

RESULTS

DFO Affects the Morphology, Numbers, and Functions of Mitochondria in a Normal Human Hepatocyte Cell Line, Chang Cells

We first attempted to determine whether the water-soluble iron chelator, DFO, exerted any significant influence on mitochondria in a normal human hepatocyte cell line, Chang cells. Treatment with 0.5 mM DFO for 3 days caused a change in the morphology of the cells. They became flat and evidenced a senescence-reminiscent morphology, as well as G1 phase cell cycle arrest (data not shown). In addition, DFO affected a reduction in the number of mitochondria, and increased the relative ratio of mitochondrial length as compared with control, according to the results of electron microscopic analysis (Fig. 1A–C). We surmised that these morphological alterations in mitochondria might accompany functional mitochondrial aberrations. We concluded that these morphological alterations in mitochondria might lead to aberrations in mitochondrial functions such as MTT activity. We found that DFO induced a time-dependent decrease in MTT activity, which remained approximately 20% for 3 days (Fig. 1D). We then attempted to determine whether mitochondrial membrane integrity was altered by DFO treatment. For this, we determined mitochondrial membrane potential (MMP, $\Delta\Psi m$) via JC-1 dye staining after 1, 2, and 3 days of either DFO treatment, or untreated (control) incubation. Since JC-1 exists in monomeric form at low membrane potential and forms red-fluorescent J-aggregates at higher potentials, it is generally employed as a sensitive marker for mitochondrial membrane potential. DFO disrupted $\Delta\Psi m$ (Fig. 1E). Subsequently, we measured ROS levels using DCF-DA in DFO-treated Chang cells. DFO induced ROS generation in the Chang cells (Fig. 1F). We then examined whether the levels of Cav-1 protein, a senescence marker protein, were consistently affected by DFO along with increases in ROS generation and changes in cellular morphology. We found that Cav-1 protein levels increased in a time-dependent manner as the result of DFO treatment (Fig. 1G). From these results, we concluded that DFO-mediated iron chelation results in mitochondrial dysfunctions as well as cellular morphological changes in Chang cells.

DFO Specifically Reduces mRNA and Protein Levels of TRAP1 and not Other Mitochondrial HSPs

Our finding that DFO induces alterations in morphology, $\Delta\Psi m$, and ROS generation in mitochondria led us to question whether DFO might affect mitochondrial HSPs, most notably, HSP60, Mot-2, and TRAP1. We analyzed mitochondrial HSP levels via Western blotting with anti-TRAP1, anti-Mot-2, and anti-HSP60 antibodies, after the DFO treatment for 3 days in Chang cells. Figure 2A shows that the levels of TRAP1 protein were specifically reduced among mitochondrial HSPs. Additionally, a decrease in TRAP1 levels was also observed at the mRNA level, as compared with Mot-2 and HSP60 levels (Fig. 2B). Thus, it appears that among mitochondrial HSPs studied, TRAP1 levels are specifically attenuated by DFO, and not Mot-2 or HSP60.

DFO-Induced Decrease in TRAP1 is Time- and Dose-Dependent

Next, we attempted to determine whether the observed reductions in the cellular levels of TRAP1 are dependent on DFO exposure time and dosage. After treating Chang cells with for 2–3 days, Western blotting against TRAP1 was conducted, and the results indicated a time-dependent reduction (Fig. 3A). DFO treatment (at a concentration of 0.05, 0.1, 0.5, and 1.0 mM, respectively) induced dose-dependent reduction in the levels of TRAP1 protein (Fig. 3B). We also tested whether the observed decreases in the levels of TRAP1 expression could be reversed by the removal of the DFO. After 0.5 mM DFO treatment for indicated periods, media was suctioned, washed with PBS twice, and replaced with fresh media without DFO. On the fifth day, the cell lysates were prepared and analyzed via Western blotting with TRAP1 antibody. As shown in Figure 3C, the decrease in TRAP1 levels was not reversed after DFO removal. Since DFO augmented ROS generation, we surmised that the reduction in TRAP1 levels may have resulted from the increase in ROS mediated by DFO. Based on this hypothesis, we

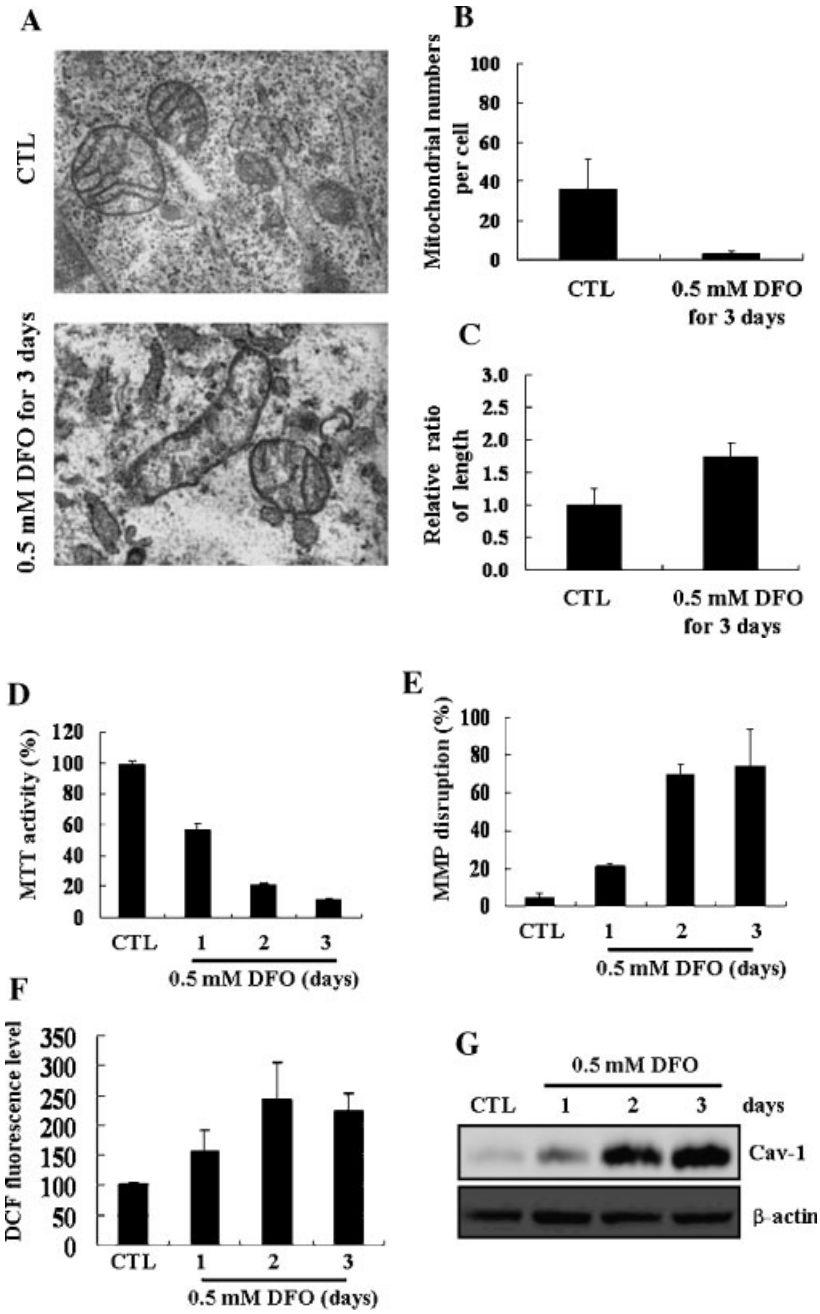

Fig. 1. Effects of deferoxamine (DFO) on the morphology, numbers and function of mitochondria in a hepatocyte cell line, Chang cells. **A**: Mitochondrial morphology affected by DFO treatment. Cells were treated without or with 0.5 mM DFO for 3 days, fixed, and analyzed via electron microscopy (×27,000). **B**: Mitochondrial numbers and relative ratio of length (**C**) to control (CTL) observed via electron microscopy. Each value is expressed as the mean ± SD from mitochondrial counts or length measurements of at least seven cells ($P < 0.05$). **D**: MTT activity. **E**: Mitochondrial membrane potential ($\Delta\Psi m$) as detected by FACS analysis after JC-1 staining. **F**: Reactive oxygen species (ROS) levels using DCF-DA fluorescent dye. **G**: Levels of caveolin-1(Cav-1) and β-actin (loading control) proteins in the absence or presence of 0.5 mM DFO in the indicated period.

examined the effects of anti-oxidant NAC, a reduced glutathione provider and a direct ROS scavenger, on the levels of TRAP1 after DFO treatment. Figure 3D indicates that NAC treatment at concentrations of 1 or 10 mM for the indicated periods did not effectively block the reduction in TRAP1 protein levels, although NAC did partially reduce the levels of Cav-1 that had been augmented by DFO treatment. These results indicate that TRAP1 expression

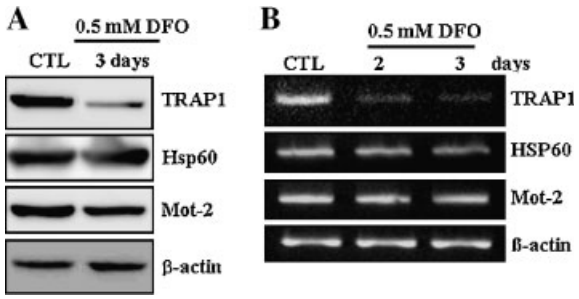

Fig. 2. Specific reduction of TRAP1 levels by DFO treatment at the mRNA and protein levels among mitochondrial HSPs. **A**: Effects of DFO on the protein levels of TRAP1, Hsp60, and Mot-2. Chang cells were grown overnight at a density of 5×10^5 cells on 100-mm dish and treated for 3 days with 0.5 mM DFO. The cell lysates were prepared and subjected to Western blotting using specific antibodies. β-actin was employed as a loading control. **B**: Effects of DFO on the mRNA levels of TRAP1, HSP60, and Mot-2. Total RNA was isolated at the indicated times, treated with DNase I, and subjected to semi-quantitative reverse transcription-PCR against TRAP1, HSP60, and Mot-2. β-actin was utilized as an internal control.

levels might not be directly regulated by ROS in DFO-treated Chang cells.

TRAP1 Levels Decreases Without Translocation From Mitochondria to Cytosol by DFO Treatment

It has been reported that TRAP1 is a mitochondrial HSP, which harbors a mitochondrial targeting leader sequence [Felts et al., 2000], although the translocation of Dd-TRAP1 from cortex of cells to mitochondria has also recently been reported [Morita et al., 2004]. In order to determine whether TRAP1 translocates from mitochondria into the cytosol by DFO treatment, cell lysates were fractionated with digitonin after incubation with or without 0.5 mM DFO for 3 days, and then Western blotting analysis against TRAP1 was conducted. Figure 4A shows that proper fractionation was achieved, as the mitochondria-specific Cox IV protein was detected only in the mitochondrial fractions. When treated with DFO, the levels of TRAP1 protein were found to be reduced in the mitochondrial fraction, while no detectable levels of TRAP1 were observed in cytosolic fraction. In addition, an immunofluorescence analysis confirmed that the decrease in TRAP1 protein levels occurs in the mitochondria, because TRAP1 was merged with MitoTracker dye in this analysis, and was time-dependently reduced by DFO. These data show that the TRAP1 levels reduced in the mitochondria without cytosolic translocation by DFO treatment.

TRAP1 Overexpression Reduces DFO-Mediated ROS Generation, Along With Decreases in SA-β-gal Activity, and Caveolin-1, Glutathione Peroxidase, and MnSOD Protein Levels

We established TRAP1-overexpressing Chang cell lines for determining whether the overexpression of TRAP1 blocks the observed

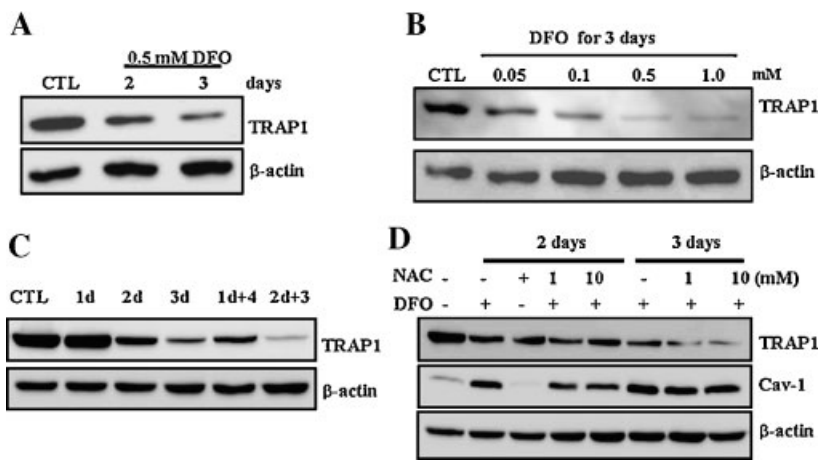

Fig. 3. Time- and dose-dependent reductions in TRAP1 levels by DFO treatment. **A**: Time-dependent reductions of TRAP1 levels by DFO treatment. After Chang cells were exposed to or unexposed to 0.5 mM DFO for 2 and 3 days, cell lysates were analyzed via Western blotting against TRAP1. **B**: Dose-dependent reductions of TRAP1 levels by DFO treatment. After DFO treatment to Chang cells at each concentration (0.05, 0.1, 0.5, and 1.0 mM) for 3 days, Western blotting for TRAP1was conducted. **C**: Levels of TRAP1 after DFO removal. Chang cells were treated with 0.5 mM DFO for the indicated periods of time (nd), and the media were replaced with fresh media without DFO for the remaining days (+n). On the fifth day, the cells were harvested and analyzed via Western blotting against TRAP1. **D**: Effects of the anti-oxidant, N-acetyl-L-cysteine (NAC) on TRAP1 and caveolin-1 (Cav-1) protein levels by DFO treatment. After NAC was treated with or without DFO for the indicated periods, Western blot analysis against TRAP1 and Cav-1 was conducted. β-actin was utilized as a loading control.

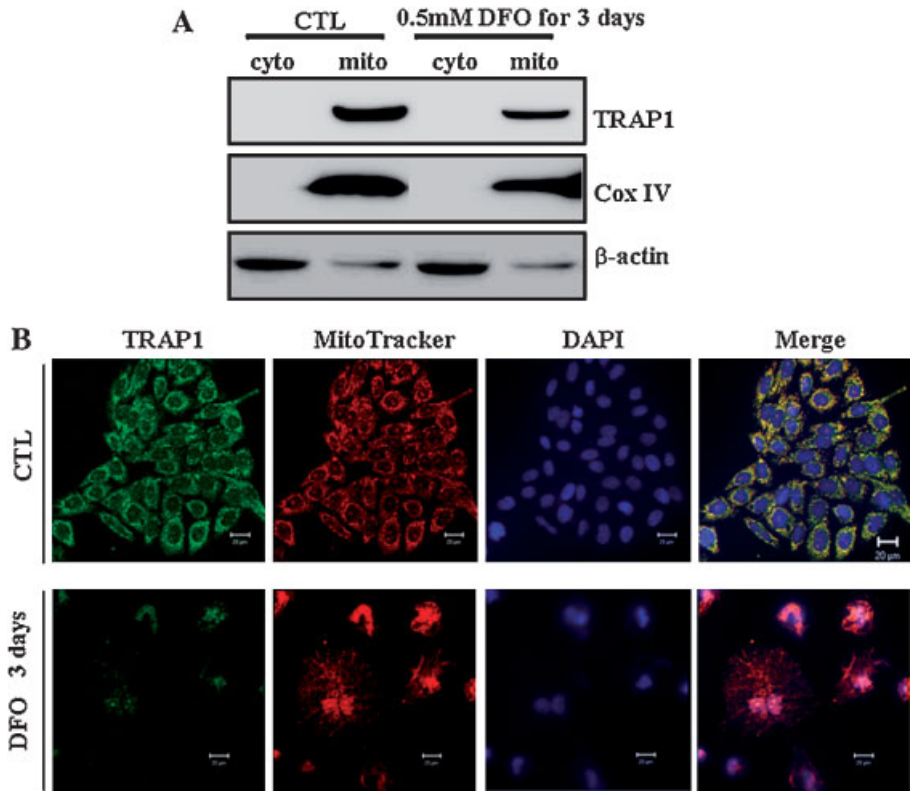

Fig. 4. Decrease of mitochondrial TRAP1 levels by DFO treatment without translocation from mitochondria to cytosol. **A**: Reduced levels of TRAP1 protein in the mitochondrial fraction. Chang cells were harvested after 3 days with or without 0.5 mM DFO, fractionated into cytosolic (cyto) and mitochondrial (mito) fractions, and subjected to Western blotting against TRAP1. Cox IV and β-actin were used as a mitochondrial marker and a loading control, respectively. **B**: Immunofluorescence analysis for TRAP1 in DFO-treated Chang cells. Cells were seeded at a density of 1×10^4 cells/well in 24-well plates, overnight after which 0.5 mM DFO was applied to the cells for the indicated times. Immunofluorescence analysis was conducted as described in the ''Materials and Methods'' (green, TRAP1; red, MitoTracker; blue, DAPI).

DFO-associated mitochondrial and cellular morphological alterations. Figure 5A indicates that the levels of TRAP1 protein in the TRAP1-transfected cells were twofold higher than those in the empty vector (EV)-transfected cells. Also, under normal conditions, overexpressed TRAP1 was localized in the mitochondria as is the case in EV-transfected cells (Fig. 5B). We subsequently assessed the levels of TRAP1 after DFO treatment for the indicated periods. We observed that in the TRAP1-transfected cells, the levels of TRAP1 were reduced by DFO in a time-dependent manner, in a pattern similar to that of the EV-transfected cells (Fig. 5C). Since the levels of TRAP1 in TRAP1-transfected cells tend to be higher than in the EV-transfected cells regardless of DFO treatment, we employed these cells in the following experiments. After the treatment of EV- or TRAP1-transfected Chang cells with 0.5 mM DFO for the indicated periods, both MTT activity and $\Delta\Psi$m were evaluated. These results showed no difference in MTT activity and $\Delta\Psi$m between the EV- and TRAP1-transfected Chang cells (Fig. 6A,B). In the next step, we examined whether the increase in ROS levels by DFO treatment is blocked in the TRAP1-transfected cells. As shown in Figure 6C, TRAP1 overexpression partially reduced DFO-induced ROS generation as compared with the EV-transfected cells ($P < 0.05$). SA-β-gal activity, known as a senescence-associated biomarker, was previously found to increase in DFO-treated Chang cells and other cells [Yoon et al., 2003, 2004]. To determine the effect of TRAP1 on SA-β-gal activity by DFO treatment, we conducted SA-β-gal staining in DFO-treated EV or TRAP1 cells. Increased SA-β-gal activity by DFO treatment was significantly reduced in the TRAP1-transfected cells, compared to the EV cells for 2 and 3 days ($P < 0.05$, Fig. 6D,E). In addition, reductions of ROS-related proteins such as Cav-1, GPX, and MnSOD occurred more prominently in the DFO-treated TRAP1 cells than in

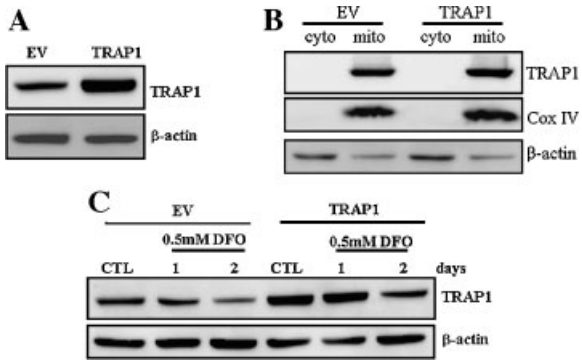

Fig. 5. Establishment of empty vector (EV) or TRAP1 transfected Chang cells. **A**: Levels of TRAP1 in EV or TRAP1 stably transfected Chang cells. As described in ''Materials and Methods'', cells selected with G418 were harvested and subjected to western blotting against TRAP1 and β-actin. **B**: TRAP1 protein levels in the mitochondrial fraction. After being cultured under normal conditions, EV or TRAP1 transfected Chang cells were prepared, fractionated into cytosolic (cyto) and mitochondrial (mito) fractions, and subjected to Western blotting against TRAP1. Cox IV and β-actin were used as a mitochondrial marker and a loading control, respectively. **C**: Time-dependent decrease of TRAP1 levels by DFO treatment in EV or TRAP1 transfected Chang cells. After DFO treatment for the indicated times, the cells were analyzed via Western blotting.

the EV cells (Fig. 6F). Taken together, it appears that TRAP1 may be involved in the regulation of DFO-induced ROS generation.

DISCUSSION

DFO, a hexadentate hydroxamate, produced by *Streptomyces pilosus* binds to iron 1:1 stoichiometrically [Keberle, 1964]. DFO inhibits or stimulates various genes including cytochrome c oxidases and ubiquinone oxidoreductase. The fact that these genes are involved in energy production, may explain why iron chelation decreases cellular energy production [Ye and Connor, 1999]. HSPs have been known to protect cells from diverse stresses [Li et al., 2000; Goldberg, 2003; Masuda et al., 2004]. However, it had not been well known that effects of DFO-mediated iron chelation on the mitochondrial HSPs. The present study shows that DFO specifically reduces levels of TRAP1, a mitochondrial HSP, and that decrease of TRAP1 levels may be involved in ROS generation induced by DFO treatment.

DFO caused G1 arrest, and altered the morphology of Chang cells, leading to a flattened

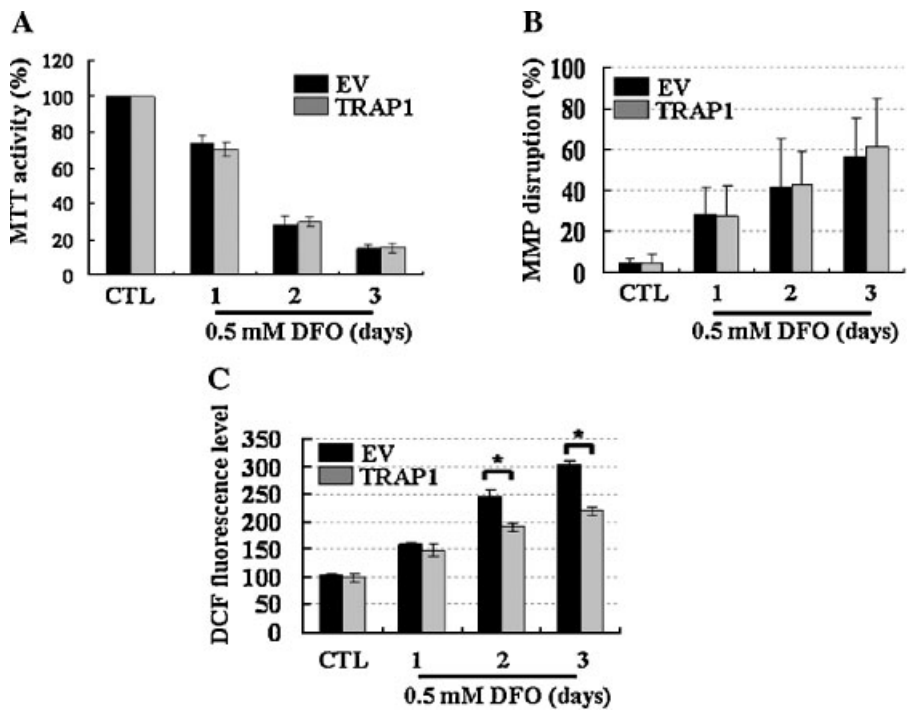

Fig. 6. MTT activity (**A**), MMP disruption (**B**), and ROS level (**C**) in DFO-treated EV or TRAP1 transfected Chang cells. Each value is expressed as mean ± SD. **D** and **E**: Senescence-associated β-gal activity by DFO treatment in EV or TRAP1 transfected Chang cells. The SA-β-gal stained cells were photographed via microscopy (×200). The strongly stained cells were considered positive, counted, and represented as a percentage of the total number of cells. Each value is expressed as mean ± SD (*$P < 0.05$). **F**: Protein levels of MnSOD, GPX, and Cav-1 in the DFO-treated EV or TRAP1 transfected cells. Cu/ZnSOD was used as a loading control.

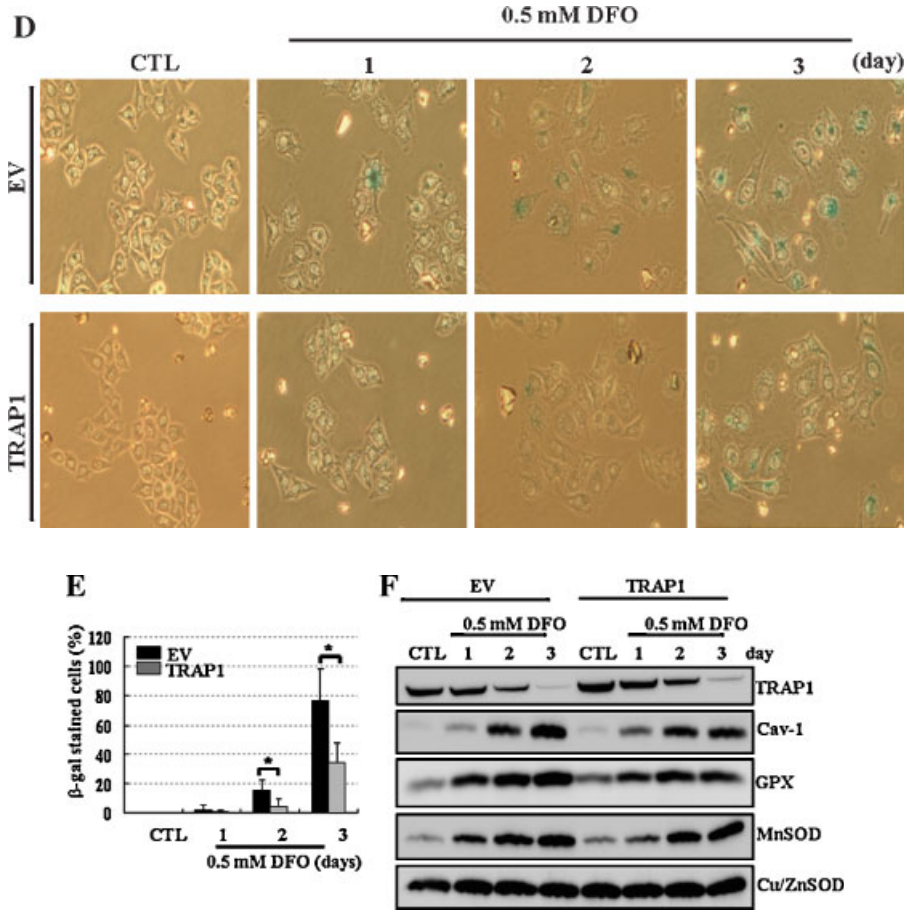

Fig. 6. (*Continued*)

shape seen in senescence (data not shown). Moreover, DFO decreased the number of mitochondria, and increased their length, as determined by our electron microscopy. Mitochondria continuously undergo fission and fusion upon normal condition and diverse stresses. These dynamics of mitochondria play an important role in cellular function. For example, mitochondria often fragment upon apoptosis induction [Wolter et al., 1997; Green and Reed, 1998; Suzuki et al., 2000; Frank et al., 2001]. As opposed to the fission, mitochondrial fusion has been implicated as a defense process against mitochondrial dysfunction with age [Ono et al., 2001]. In this regard, it seems likely that elongation of mitochondria makes genetic contents between them exchange upon DFO treatment [Yoon et al., 2004]. It might be possible that cells under stress are partially protected from mitochondrial dysfunction by complementation of mitochondrial DNA via fusion. These alterations in mitochondria were accompanied by functional decreases such as reduced MTT activity and disruptions of mitochondrial membrane integrity (Fig. 1), consistent with other recent reports [Brodie et al., 1993; Yoon et al., 2003, 2004]. Also, the levels of Cav-1, a known marker for senescence [Volonte et al., 2002] were increased by DFO treatment, coupled with ROS accumulation (Fig. 1F,G). Interestingly, we observed that DFO dramatically decreased TRAP1 levels, but not the levels of HSP60 and Mot-2, as compared with controls. This decrease occurred at both the mRNA and protein levels. The levels of TRAP1 were decreased in a dose- and time-dependent manner by DFO treatment. Also once TRAP1 was decreased by DFO, removal of DFO did not lead to a restoration of original TRAP1 levels (Fig. 3C). This irreversible DFO-induced reduction in TRAP1 levels is consistent with the previous findings that DFO causes irreversible G1 arrest and ATP level reductions [Yoon et al., 2003, 2004].

TRAP1 levels were decreased without translocation from mitochondria to cytosol by DFO

treatment, as shown in our immunofluorescence and subcellular fractionation analyses. A recent report [Masuda et al., 2004] suggested that levels of TRAP1 expression might be regulated by ROS levels in β-HIVS-induced apoptosis. In our study the anti-oxidant, NAC, did not block the attenuation of TRAP1 levels by DFO, while DFO-induced reduction in Cav-1 levels still occurred (Fig. 3D). However, TRAP1 overexpression affected a partial blockage of DFO-induced ROS generation, thereby delaying senescence-associated characteristics, including SA-β-gal activity and increases in the levels of Cav-1 (Fig. 6C–F). This indicates that TRAP1 might be associated with the upstream pathway of ROS regulation.

ROS is highly reactive O_2 metabolites that include superoxide radical, hydrogen peroxide (H_2O_2), and hydroxyl radical (OH). It has been known that sources of cellular ROS include mitochondria, plasma membrane as well as peroxisomes [Moldovan and Moldovan, 2004]. Based on our results, it seems likely that ROS is mainly released from mitochondria upon DFO treatment because of following reasons. Firstly, while levels of Cu/ZnSOD mostly in the cytoplasm did not increase, those of MnSOD in largely mitochondrial matrix increased upon DFO treatment (Fig. 6F). Secondly, because we observed that TRAP1 is localized to mitochondria and ROS levels decreased in TRAP1-transfected Chang cells, ROS might be released from mitochondria upon DFO treatment. However, considering partial effect of TRAP1 on ROS levels, some ROS levels might be release from other sources. ROS has been known as a second messenger in cellular processes such as apoptosis, differentiation, and senescence [Inoue et al., 2004; Sauer and Wartenberg, 2005]. Since SA-β-gal activity has been reported by Dimri et al. [1995], it has been used as a biomarker of senescence and aging. While most cells express a lysosomal β-galactosidase, that is, detected by X-Gal at about pH 4, only senescent cells are stained at pH 6 [Dimri et al., 1995]. Our observation that SA-β-gal activity decreased upon DFO treatment in TRAP1-transfected Chang cells might provide a clue that TRAP1 is involved in aging-related disorders [Bondy, 1992; Sohal and Weindruch, 1996; Men'shchikova et al., 2002].

We found no difference in MTT activity or MMP disruption, although ROS levels decreased upon DFO treatment in TRAP1-transfected cells compared with EV-transfected cells. It has been reported that MMP disruption occurs with ROS increase during apoptosis [Zamzami et al., 1995; Herrera et al., 2001]. However, we determined MTT activity, MMP disruption and ROS levels in senescence-like system by DFO treatment, but not in apoptosis system. Therefore, these might be dependent on stimuli and cell types. On the other hand, it is possible that the mechanism that TRAP1 regulates ROS levels might be independent of those of MTT activity and MMP disruption upon DFO treatment.

TRAP1 had been initially identified as a novel protein, exhibiting homology with HSP90, which binds to the intracellular domain of the type I TNF receptor and is variably expressed in mammalian tissues and cancer cell lines [Song et al., 1995]. TRAP1 has been shown to bind to retinoblastoma protein (Rb) during heat shock and mitosis events [Chen et al., 1996]. Although it is a member of the HSP90 family, TRAP1 may be functionally distinct from HSP90 [Felts et al., 2000]. As ROS is physiologically generated via oxidative phosphorylation [Miyamoto et al., 2003], TRAP1 seems to play a role in regulating ROS and maintaining the homeostasis. Some diseases have been associated with ROS dysregulation [Mates and Sanchez-Jimenez, 1999; Calabrese et al., 2005]. In this regard, our results might provide a clue for a link between TRAP1 and ROS-related pathogenesis.

In summary, our study suggests that the DFO dramatically decreased TRAP1 levels, coupled with ROS generation and that TRAP1 may be involved in the regulation of ROS. The manner in which TRAP1 expression is regulated, the nature of the substrate to which TRAP1 binds, and the mechanism by which TRAP1 regulates ROS in the mitochondria, are all questions which will, hopefully, be resolved in future research.

ACKNOWLEDGMENTS

We thank our laboratory members including Sun-Hye Kim for their inspiration during this study. This work was supported in part by 2005 BK21 project for Medicine, Dentistry and Pharmacy to Chang-Nim Im and Jeong-Sun Seo.

REFERENCES

Alcantara O, Obeid L, Hannun Y, Ponka P, Boldt DH. 1994. Regulation of protein kinase C (PKC) expression by iron:

Effect of different iron compounds on PKC-beta and PKC alpha gene expression and role of the 5′ flanking region of the PKC-beta gene in the response to ferric transferrin. Blood 84:3610–3617.

Bondy SC. 1992. Reactive oxygen species: Relation to aging and neurotoxic damage. Neurotoxicology 13:87–100.

Brodie C, Siriwardana G, Lucas J, Schleicher R, Terada N, Szepesi A, Gelfand E, Seligman P. 1993. Neuroblastoma sensitivity to growth inhibition by deferrioxamine: Evidence for a block in G1 phase of the cell cycle. Cancer Res 53:3968–3975.

Cabiscol E, Belli G, Tamarit J, Echave P, Herrero E, Ros J. 2002. Mitochondrial Hsp60, resistance to oxidative stress, and the labile iron pool are closely connected in Saccharomyces cerevisiae. J Biol Chem 277:44531–44538.

Calabrese V, Lodi R, Tonon C, D'Agata V, Sapienza M, Scapagnini G, Mangiameli A, Pennisi G, Stella AM, Butterfield DA. 2005. Oxidative stress, mitochondrial dysfunction and cellular stress response in Friedreich's ataxia. J Neurol Sci 233:145–162.

Chen CF, Chen Y, Dai K, Chen PL, Riley DJ, Lee WH. 1996. A new member of the hsp90 family of molecular chaperones interacts with the retinoblastoma protein during mitosis and after heat shock. Mol Cell Biol 16: 4691–4699.

Dimri GP, Lee X, Basile G, Acosta M, Scott G, Roskelley C, Medrano EE, Linskens M, Rubelj I, Pereira-Smith O, et al. 1995. A biomarker that identifies senescent human cells in culture and in aging skin in vivo. Proc Natl Acad Sci USA 92:9363–9367.

Fan L, Iyer J, Zhu S, Frick KK, Wada RK, Eskenazi AE, Berg PE, Ikegaki N, Kennett RH, Frantz CN. 2001. Inhibition of N-myc expression and induction of apoptosis by iron chelation in human neuroblastoma cells. Cancer Res 61:1073–1079.

Felts SJ, Owen BA, Nguyen P, Trepel J, Donner DB, Toft DO. 2000. The hsp90-related protein TRAP1 is a mitochondrial protein with distinct functional properties. J Biol Chem 275:3305–3312.

Frank S, Gaume B, Bergmann-Leitner ES, Leitner WW, Robert EG, Catez F, Smith CL, Youle RJ. 2001. The role of dynamin-related protein 1, a mediator of mitochondrial fission, in apoptosis. Dev Cell 1:515–525.

Goldberg AL. 2003. Protein degradation and protection against misfolded or damaged proteins. Nature 426: 895–899.

Green DR, Reed JC. 1998. Mitochondria and apoptosis. Science 281:1309–1312.

Hatefi Y. 1985. The mitochondrial electron transport and oxidative phosphorylation system. Annu Rev Biochem 54:1015–1069.

Herrera B, Alvarez AM, Sanchez A, Fernandez M, Roncero C, Benito M, Fabregat I. 2001. Reactive oxygen species (ROS) mediates the mitochondrial-dependent apoptosis induced by transforming growth factor (beta) in fetal hepatocytes. Faseb J 15:741–751.

Inoue M, Sato EF, Nishikawa M, Hiramoto K, Kashiwagi A, Utsumi K. 2004. Free radical theory of apoptosis and metamorphosis. Redox Rep 9:237–247.

Keberle H. 1964. The biochemistry of desferrioxamine and its relation to iron metabolism. Ann N Y Acad Sci 119: 758–768.

Koeller DM, Horowitz JA, Casey JL, Klausner RD, Harford JB. 1991. Translation and the stability of mRNAs encoding the transferrin receptor and c-fos. Proc Natl Acad Sci USA 88:7778–7782.

Kontoghiorghes GJ, Piga A, Hoffbrand AV. 1986. Cytotoxic and DNA inhibitory effects of iron chelators on human leukaemic cells. Hematol Oncol 4:195–204.

Kuhn LC, Schulman HM, Ponka P. 1990. Iron-transferrin requirements and transferrin receptor expression in proliferating cells. In: Ponka P, Schulman HM, Woodworth RC, editors. Iron transport and storage. Boca Raton, FL: CRC Press, pp 141–191.

Lederman HM, Cohen A, Lee JW, Freedman MH, Gelfand EW. 1984. Deferoxamine: A reversible S-phase inhibitor of human lymphocyte proliferation. Blood 64:748–753.

Lee SH, Kim M, Yoon BW, Kim YJ, Ma SJ, Roh JK, Lee JS, Seo JS. 2001. Targeted hsp70.1 disruption increases infarction volume after focal cerebral ischemia in mice. Stroke 32:2905–2912.

Li CY, Lee JS, Ko YG, Kim JI, Seo JS. 2000. Heat shock protein 70 inhibits apoptosis downstream of cytochrome c release and upstream of caspase-3 activation. J Biol Chem 275:25665–25671.

Liu Y, Liu W, Song XD, Zuo J. 2005. Effect of GRP75/mthsp70/PBP74/mortalin overexpression on intracellular ATP level, mitochondrial membrane potential and ROS accumulation following glucose deprivation in PC12 cells. Mol Cell Biochem 268:45–51.

Masuda Y, Shima G, Aiuchi T, Horie M, Hori K, Nakajo S, Kajimoto S, Shibayama-Imazu T, Nakaya K. 2004. Involvement of tumor necrosis factor receptor-associated protein 1 (TRAP1) in apoptosis induced by beta-hydroxyisovalerylshikonin. J Biol Chem 279:42503–42515.

Mates JM, Sanchez-Jimenez F. 1999. Antioxidant enzymes and their implications in pathophysiologic processes. Front Biosci 4:D339–D345.

Men'shchikova EB, Shabalina IG, Zenkov NK, Kolosova NG. 2002. Generation of reactive oxygen species by mitochondria in senescence-accelerated OXYS rats. Bull Exp Biol Med 133:175–177.

Miyamoto Y, Koh YH, Park YS, Fujiwara N, Sakiyama H, Misonou Y, Ookawara T, Suzuki K, Honke K, Taniguchi N. 2003. Oxidative stress caused by inactivation of glutathione peroxidase and adaptive responses. Biol Chem 384:567–574.

Moldovan L, Moldovan NI. 2004. Oxygen free radicals and redox biology of organelles. Histochem Cell Biol 122:395–412.

Morita T, Amagai A, Maeda Y. 2002. Unique behavior of a dictyostelium homologue of TRAP-1, coupling with differentiation of D. discoideum cells. Exp Cell Res 280:45–54.

Morita T, Amagai A, Maeda Y. 2004. Translocation of the Dictyostelium TRAP1 homologue to mitochondria induces a novel prestarvation response. J Cell Sci 117:5759–5770.

Morita T, Yamaguchi H, Amagai A, Maeda Y. 2005. Involvement of the TRAP-1 homologue, Dd-TRAP1, in spore differentiation during Dictyostelium development. Exp Cell Res 303:425–431.

Nyholm S, Mann GJ, Johansson AG, Bergeron RJ, Graslund A, Thelander L. 1993. Role of ribonucleotide reductase in inhibition of mammalian cell growth by potent iron chelators. J Biol Chem 268:26200–26205.

Oexle H, Gnaiger E, Weiss G. 1999. Iron-dependent changes in cellular energy metabolism: Influence on

citric acid cycle and oxidative phosphorylation. Biochim Biophys Acta 1413:99–107.

Ono T, Isobe K, Nakada K, Hayashi JI. 2001. Human cells are protected from mitochondrial dysfunction by complementation of DNA products in fused mitochondria. Nat Genet 28:272–275.

Richardson DR, Baker E. 1990. The uptake of iron and transferrin by the human melanoma cell. Biochim Biophys Acta 1053:1–12.

Robbins E, Pederson T. 1970. Iron: Intracellular localization and possible role in cell division. Proc Natl Acad Sci USA 66:1244–1251.

Saraste M. 1999. Oxidative phosphorylation at the *fin de siecle*. Science 283:1488–1493.

Sauer H, Wartenberg M. 2005. Reactive oxygen species as signaling molecules in cardiovascular differentiation of embryonic stem cells and tumor-induced angiogenesis. Antioxid Redox Signal 7:1423–1434.

Shim EH, Kim JI, Bang ES, Heo SJ, Lee JS, Kim EY, Lee JE, Park WY, Kim SH, Kim HS, Smithies O, Jang JJ, Jin DI, Seo JS. 2002. Targeted disruption of hsp70.1 sensitizes to osmotic stress. EMBO Rep 3:857–861.

Sohal RS, Weindruch R. 1996. Oxidative stress, caloric restriction, and aging. Science 273:59–63.

Song HY, Dunbar JD, Zhang YX, Guo D, Donner DB. 1995. Identification of a protein with homology to hsp90 that binds the type I tumor necrosis factor receptor. J Biol Chem 270:3574–3581.

Suzuki M, Youle RJ, Tjandra N. 2000. Structure of Bax: Coregulation of dimer formation and intracellular localization. Cell 103:645–654.

Volonte D, Zhang K, Lisanti MP, Galbiati F. 2002. Expression of caveolin-1 induces premature cellular senescence in primary cultures of murine fibroblasts. Mol Biol Cell 13:2502–2517.

Weiss G., Werner-Falmayer G, Werner ER, Grunewald K, Wachte H. 1994. Iron regulates nitric oxide synthase activity by controlling nuclear transcription. J Exp Med 180:969–976.

Wolter KG, Hsu YT, Smith CL, Nechushtan A, Xi XG, Youle RJ. 1997. Movement of Bax from the cytosol to mitochondria during apoptosis. J Cell Biol 139:1281–1292.

Ye Z, Connor JR. 1999. Screening of transcriptionally regulated genes following iron chelation in human astrocytoma cells. Biochem Biophys Res Commun 264:709–713.

Yoon YS, Byun HO, Cho H, Kim BK, Yoon G. 2003. Complex II defect via down-regulation of iron-sulfur subunit induces mitochondrial dysfunction and cell cycle delay in iron chelation-induced senescence-associated growth arrest. J Biol Chem 278:51577–51586.

Yoon YS, Cho H, Lee JH, Yoon G. 2004. Mitochondrial dysfunction via disruption of complex II activity during iron chelation-induced senescence-like growth arrest of Chang cells. Ann N Y Acad Sci 1011:123–132.

Zamzami N, Marchetti P, Castedo M, Decaudin D, Macho A, Hirsch T, Susin SA, Petit PX, Mignotte B, Kroemer G. 1995. Sequential reduction of mitochondrial transmembrane potential and generation of reactive oxygen species in early programmed cell death. J Exp Med 182:367–377.